Coda wave interferometry and the equilibration of energy in elastic media

Roel Snieder
Department of Geophysics and Center for Wave Phenomena, Colorado School of Mines, Golden, Colorado 80401
(Received 14 May 2002; published 21 October 2002)

Multiple-scattered waves usually are not useful for creating deterministic images of the interior of elastic media. However, in many applications, one is not so much interested in making a deterministic image as in detecting changes in the medium. Cases in point are volcano monitoring and measuring the change in hydrocarbon reservoirs during enhanced recovery operations. Coda wave interferometry is a technique wherein changes in multiple-scattered waves are used as a diagnostic for minute changes in the medium. This technique was developed previously for scalar waves; however, the application of this technique in geophysics, nondestructive testing, and other applications where elastic waves are used, requires the extension of the existing formulation of coda wave interferometry to include conversions between *P* and *S* waves. Here, a simple model for the equilibration between *P* and *S* waves incorporates into the theory of coda wave interferometry the mode conversions that are inherent to multiply scattered elastic waves.

DOI: 10.1103/PhysRevE.66.046615 PACS number(s): 42.25.Fx, 03.65.Nk, 91.30.−f

I. INTRODUCTION

Imaging techniques, as used in seismic imaging [1], nondestructive testing [2], radar applications, and medical imaging [3], usually rely on a single-scattering approximation. In many practical applications waves are strongly scattered, and deterministic imaging is not feasible. Often, however, the primary goal is not to form an image of the interior of a medium, but to detect changes in the medium instead.

Speckle pattern interferometry [4–7] uses the change in the spatial speckle pattern of interfering multiply scattered waves to retrieve the average change in the scatterer locations as a result of changes in the medium. This technique has been used to monitor Brownian motion in colloidal suspensions [8], the passage of ultrasound through a strongly scattering medium [9], and the properties of Taylor-Couette flow [10]. Speckle pattern interferometry requires the measurement of the intensity of the wave field over a certain region of space. Although this is straightforward when light waves are used, spatial sampling is a problem in situations where the wave field or its intensity can be measured only at a limited number of locations.

When only a limited number of detectors of the wave field are in place, one can use the temporal fluctuations of the transient multiple-scattered waves. The idea is to exploit the change in the multiple-scattered waves generated by a transient incident wave as a diagnostic of the change in the medium. The term "coda" is used to denote the relatively late-arriving multiply scattered waves; this term comes from music where it denotes the closing passage of the piece. The technique to extract the change in the medium from the change in the multiple scattered waves is called "coda wave interferometry" [11] because the multiple-scattering medium acts as an interferometer.

Coda wave interferometry can potentially be used in nondestructive testing of materials to detect the formation of cracks, but it also has applications for monitoring changes in hydrocarbon and hydrological reservoirs, and for the monitoring of dams and volcanoes. In such applications, the number of receivers is often limited, so that the temporal speckle pattern of the multiple-scattered waves is the primary tool to detect changes in the medium.

Because for these applications the medium is elastic, the theory developed for coda wave interferometry of scalar waves [11] is not applicable. A number of seismological studies have been carried out to infer a change in the seismic velocity from coda waves [12–16]. In an elastic medium there is not a single wave velocity because such a medium supports both *P* and *S* waves, each with a distinct velocity. In strongly scattering elastic media, conversions between *P* and *S* waves are in general as strong as the scattering of these waves. Since a multiply scattered wave has traveled over part of its trajectory as a *P* wave and part of its trajectory as an *S* wave, it is not obvious how often an elastic wave at a given time has been scattered and what the effective velocity of propagation is. Aki and Chouet [17] assume that the coda waves are dominated by *S* waves.

Here, I extend the theory of coda wave interferometry [11] for scalar waves to the more complex application of elastic waves. Section II treats multiple scattering of vector waves, and the influence of changes in the medium on these waves. To account for the partitioning of propagation between *P* and *S* waves, I introduce a simple model for the propagation of elastic waves in Secs. III and IV. The information on the spatial distribution and directionality of the waves is discarded in this model, which results in a simple description of the partitioning of *P*- and *S*-wave energies. With this model, I infer the change in the coda waves due to a change in the scatterer locations (Sec. V) and the propagation velocity (Sec. VI).

II. PERTURBATION OF THE MULTIPLE-SCATTERED WAVES

Let us assume that discrete scatterers in the medium strongly scatter elastic waves. When the separation between the scatterers is much larger than a wavelength, the total wave field can be written as the sum of waves that propagate along all possible trajectories:

$$\mathbf{u}^{(u)}(t)=\sum_T \mathbf{A}_T(t). \tag{1}$$

A trajectory is defined as a sequence of scatterers through which the wave has traveled over time. At each scatterer, conversions between P and S waves can occur. The sum over trajectories also enumerates all the possible combinations of modes of propagation as P and S waves between consecutive scatterers that are encountered.

The wave field in Eq. (1) is the wave field for the unperturbed medium; this is called the unperturbed wave field. Let us assume that, when the medium is perturbed, the dominant action of this perturbation is to change the travel time along each trajectory, and that the change in the (vector) amplitude can be ignored. Denoting the travel time perturbation for the propagation along trajectory T by τ_T, we can therefore write the perturbed wave field as

$$\mathbf{u}^{(p)}(t)=\sum_T \mathbf{A}_T(t-\tau_T). \tag{2}$$

Suppose that one has measured the i component of the unperturbed and perturbed wave fields. We characterize the change in the wave field using the time-windowed correlation function, defined as

$$C_{up}^{(t,t_w)}(t_s)\equiv\int_{t-t_w}^{t+t_w} u_i^{(u)}(t')u_i^{(p)}(t'+t_s)dt', \tag{3}$$

where t denotes the center of a time window of length $2t_w$ and t_s the lag time for the correlation. The cross correlation is given by

$$C_{up}^{(t,t_w)}(t_s)\equiv\sum_{TT'}\int_{t-t_w}^{t+t_w} A_{Ti}(t')A_{T'i}(t'+t_s-\tau_{T'})dt'. \tag{4}$$

The double sum over all trajectories can be written as $\Sigma_{TT'}=\Sigma_{T=T'}+\Sigma_{T\neq T'}$. The terms in the first sum add coherently, while the terms in the second sum add incoherently. For this reason the contribution of the trajectories $T\neq T'$ can be neglected; hence

$$C_{up}^{(t,t_w)}(t_s)=\sum_T\int_{t-t_w}^{t+t_w} A_{Ti}(t')A_{Ti}(t'+t_s-\tau_T)dt'. \tag{5}$$

In the following we consider a shift time t_s that is close to the mean travel time perturbation. For small values of $(t_s-\tau_T)$ a second order Taylor expansion of $A_{Ti}(t'+t_s-\tau_T)$ gives

$$C_{up}^{(t,t_w)}(t_s)=\sum_T\int_{t-t_w}^{t+t_w} A_{Ti}(t')^2dt' + \frac{1}{2}\sum_T (t_s-\tau_T)^2\int_{t-t_w}^{t+t_w} A_{Ti}(t')\ddot{A}_{Ti}(t')dt'. \tag{6}$$

This expression can be written as

$$C_{up}^{(t,t^w)}(t_s)=\sum_T\int_{t-t_w}^{t+t_w} A_{Ti}(t')^2dt'\left(1-\frac{1}{2}\overline{\omega^2}(t_s-\tau_T)^2\right), \tag{7}$$

with the dominant frequency defined as

$$\overline{\omega^2}\equiv-\frac{\Sigma_T\int_{t-t_w}^{t+t_w}A_{Ti}(t')\ddot{A}_{Ti}(t')dt'}{\Sigma_T\int_{t-t_w}^{t+t_w}A_{Ti}(t')^2dt'}. \tag{8}$$

Analogous to Eq. (3), the zero-lag time-windowed autocorrelation of the unperturbed wave is defined as

$$C_{uu}^{(t,t_w)}(0)\equiv\int_{t-t_w}^{t+t_w} u_i^{(u)2}(t')dt', \tag{9}$$

with a similar definition for $C_{pp}^{(t,t_w)}(0)$ for the perturbed waves. Using a similar reasoning as used in deriving expression (5) gives

$$C_{uu}^{(t,t_w)}(0)=C_{pp}^{(t,t_w)}(0)=\sum_T\int_{t-t_w}^{t+t_w} A_{Ti}^2(t')dt'. \tag{10}$$

A dimensionless measure of the change of the wave field is given by the time-windowed correlation coefficient defined as

$$R^{(t,t_w)}(t_s)\equiv\frac{\int_{t-t_w}^{t+t_w}u_i^{(u)}(t')u_i^{(p)}(t'+t_s)dt'}{\left(\int_{t-t_w}^{t+t_w}u_i^{(u)2}(t')dt'\int_{t-t_w}^{t+t_w}u_i^{(p)2}(t')dt'\right)^{1/2}}. \tag{11}$$

With the expressions (7) and (10), this function is approximately given by

$$R^{(t,t_w)}(t_s)=1-\frac{1}{2}\overline{\omega^2}\langle(\tau-t_s)^2\rangle_{(t,t_w)}. \tag{12}$$

In this expression, $\langle\cdots\rangle_{(t,t_w)}$ denotes the average over all trajectories that arrive in the time window $(t-t_w,t+t_w)$ with a weight factor that is given by A_{Ti}^2. This means that in this work averages are taken with a weight factor that is given by the energy of each multiple-scattered wave.

The time shifted cross correlation attains its maximum when

$$t_s=\langle\tau\rangle_{(t,t_w)}, \tag{13}$$

and the value of the time shifted cross correlation at its maximum satisfies

$$R_{\max}^{(t,t_w)}=1-\frac{1}{2}\overline{\omega^2}\sigma_\tau^2, \tag{14}$$

with σ_τ the variance of the perturbation of the arrival times in the employed time window. This means that the time shifted cross correlation of the unperturbed and the perturbed waves gives the mean and variance of the travel time perturbation in the employed time window.

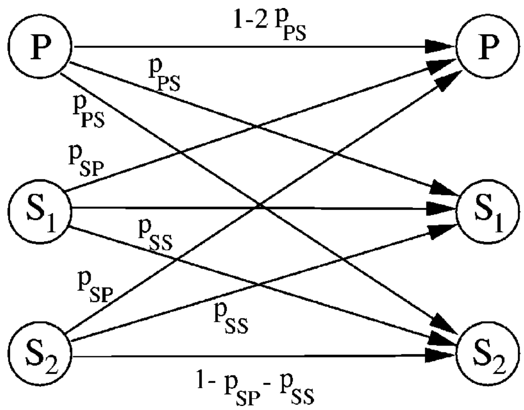

FIG. 1. Diagrammatic representation of the transition probabilities for the conversions of balls among the P state and the two S states.

III. A SIMPLE EQUILIBRATION MODEL FOR *P* AND *S* WAVES

The mean and variance of the arrival times of seismic waves for a given perturbation of the medium is the result of the change in the propagation of both P and S waves because each trajectory consists of a combination of paths between scatterers along which the wave travels as a P or S wave. To make further progress, it is necessary to account for the partitioning of elastic wave energy into P and S energy.

The partitioning of P-wave energy to S-wave energy has been studied by counting the number of P and S modes [18], from the evolution equations for P- and S-wave energy [19], from radiative transfer theory [20,21], and from seismological observations [22]. The temporal evolution of the P- and S-wave energies in an elastic medium can be studied with a hierarchy of different methods. In radiative transfer theory [20,23–27], the spatial distributions of the intensity and the direction of propagation are treated as independent parameters. When the transition to diffusive wave propagation is made, the direction of energy propagation is related to the gradient of the intensity [21,28].

As an alternative I use in this section an even simpler model to account for the equilibration of P and S waves where the information regarding the spatial distribution and direction of the waves is discarded. In this model, the waves move around as balls. A ball is either in a P state, or in the S_1 and S_2 states that represent the two polarizations of S waves. The balls are a metaphor for units of energy. However, the balls should not be confused with the quanta of elastic wave propagation (phonons); they are nothing but a tool for keeping track of the distribution of energy among the different wave modes. The balls in the P state travel with the P-wave velocity v_P, while the balls in the S states travel with the S-wave velocity v_S. After each ball has propagated over a distance a, with a certain probability it can convert to a ball of another state. The model is similar to a Monte Carlo description of multiple scattering [29,30], but spatial and directional information about the propagation of the waves is discarded. This allows for an analytical solution rather than a numerical solution based on a Monte Carlo technique.

The probabilities of these transitions are shown in Fig. 1. The probability that a P ball converts to each of the S states is denoted by p_{PS}. This means that the probability at each collision that a P ball continues as a P ball is equal to $1-2p_{PS}$. The probability that an S ball is converted into a P ball at a scatterer is denoted by p_{SP}. There is a probability p_{SS} that an S ball is converted to an S ball of the other type. It follows from Fig. 1 that the probability that an S ball is not converted to a ball of another type is $1-p_{SP}-p_{SS}$.

Suppose that in the system there are N_P balls in the P state and N_{S_1} and N_{S_2} balls in the S_1 and S_2 states, respectively. The transition probabilities can be used to derive differential equations for the number of balls in each state. As an example, consider the number of balls in the P state. There are N_P balls in this state. In a time interval dt, each ball travels a distance $v_P dt$ and encounters $v_P dt/a$ scatterers. As indicated in Fig. 1, the probability that a ball in the P state is converted to each of the S states upon encountering a scatterer is p_{PS}. This means that in a time interval dt the total reduction of the P balls due to conversion to S states is given by $-2p_{PS}N_P v_P dt/a$. The number of P balls increases due to the conversion of S balls to P balls. By the same reasoning the number of balls in the P state thus increases in the same interval as $p_{SP}(N_{S_1}+N_{S_2})v_S dt/a$. The total change in the number of balls in the P state is therefore given by $dN_p = p_{SP}(N_{S_1}+N_{S_2})v_S dt/a - 2p_{PS}N_P v_P dt/a$. The same reasoning can be applied to the balls in each of the S states; this gives the following system of differential equations:

$$\dot{N}_P = \frac{1}{a}(p_{SP}v_S N_{S_1} + p_{SP}v_S N_{S_2} - 2p_{PS}v_P N_P),$$

$$\dot{N}_{S_1} = \frac{1}{a}[p_{SS}v_S N_{S_2} + p_{PS}v_P N_P - (p_{SP}+p_{SS})v_S N_{S_1}],$$

$$\dot{N}_{S_2} = \frac{1}{a}[p_{SS}v_S N_{S_1} + p_{PS}v_P N_P - (p_{SP}+p_{SS})v_S N_{S_2}]. \tag{15}$$

The average distance between scatterers is a, but this distance is not the mean free path. In the following, we take the limit that a and the transition probabilities p_{PS}, p_{SP}, and p_{SS} go to zero; this limit describes the continuous conversion between different wave types that occurs in a strongly inhomogeneous elastic medium. It follows from Fig. 1 that, when a ball in the P state encounters a scatterer, the probability that it is not converted to one of the S states is given by $1-2p_{PS}$. Since p_{PS} is assumed to be small, this means that the probability that a P ball is not converted to another state when it propagates over a distance l is given by $(1-2p_{PS})^{l/a}$. By definition, this probability is equal to $1/e$ when the ball has propagated over the mean free path l_P; hence $(1-2p_{PS})^{l_P/a}=1/e$. Taking the natural logarithm gives, for small values of p_{PS},

$$l_P = \frac{a}{2p_{PS}}. \tag{16}$$

For the balls in each S state, the probability that the ball is not converted at a scatterer is given by $1-p_{SP}-p_{SS}$. Using the same reasoning as for the balls in the P state, the mean free path of each S state is given by

$$l_S = \frac{a}{p_{SP}+p_{SS}}. \tag{17}$$

From these expressions, the mean free paths remain finite when the limits $a\to 0$, $p_{IJ}\to 0$ are taken as long as the ratio defined in expressions (16) and (17) remains finite. Note that the system of differential equations (15) depends only on the ratios p_{IJ}/a.

The system (15) has three different solutions, each with a characteristic decay time. Adding the three equations (15) gives

$$\frac{d}{dt}(N_P+N_{S_1}+N_{S_2})=0. \tag{18}$$

This expression states that the number of balls is constant in time; this is a consequence of the fact that the probabilities in Fig. 1 are chosen in such a way that balls are neither created nor destroyed when they encounter a scatterer. The identification of balls with units of energy means that for this system the total energy is conserved.

The total number of balls N_S in an S state is the sum of the balls in the two S states:

$$N_S \equiv N_{S_1}+N_{S_2}. \tag{19}$$

Using this relation in the first line of the system (15), and adding the last two lines of that system, gives the following system of equations that governs the partition between the total numbers of balls in the P and S states:

$$\dot{N}_P = \frac{1}{a}(p_{SP}v_S N_S - 2p_{PS}v_P N_P),$$

$$\dot{N}_S = \frac{1}{a}(2p_{PS}v_P N_P - p_{SP}v_S N_S). \tag{20}$$

It follows from this expression that, in equilibrium, the ratio of the number of balls in the P state to the total number of balls in the S states is given by

$$\left(\frac{N_P}{N_S}\right)_{\mathrm{eq}} = \frac{p_{SP}v_S}{2p_{PS}v_P}. \tag{21}$$

The ratio of the number of balls, and hence the ratio of the P- and S-wave energies depends on the ratio p_{SP}/p_{PS} of the transition probabilities. Aki [31] gives a simple derivation based on reciprocity that explains why these probabilities are different. These transition probabilities are defined in expression (15), where they multiply terms such as $v_P N_P$. When N_P denotes the P-wave energy, then $v_P N_P$ describes the energy flux of P waves. In scattering theory the scattering cross section is defined by the change in the energy flux. Therefore, the ratio p_{SP}/p_{PS} is defined by the ratio of the scattering cross sections for PS scattering and SP scattering, respectively, which is given by [30]

$$\frac{p_{SP}}{p_{PS}} = 2\frac{\sigma_{SP}}{\sigma_{PS}} = \left(\frac{v_S}{v_P}\right)^2. \tag{22}$$

The factor 2 in the middle term is due to the fact that the transition probability in Eq. (15) is defined for each S-wave polarization separately whereas the cross section σ_{SP} is defined for the total S-wave energy.

Inserting the ratio (22) in (21) and identifying the number of balls with energy, the following conditions follow for the equilibrium value of the P- and S-wave energy [18–21]:

$$\left(\frac{E_P}{E_S}\right)_{\mathrm{eq}} = \frac{1}{2}\left(\frac{v_S}{v_P}\right)^3. \tag{23}$$

For a Poisson medium, where $v_P=\sqrt{3}v_S$, this ratio is given by $(E_P/E_S)_{eq}\approx 0.096$, which indicates that the S-wave energy is much larger than the P-wave energy. There are three reasons for this. First, there are two S states compared to only one P state. Second, the P waves propagate faster than do the S waves, so the probability per unit time that a P wave is converted to an S wave is much larger than that of the reverse conversion. Third, the transition probability for the conversion from P to S is larger than from S to P; see expression (22).

Expressions (20) and (18) provide the time it takes for the number of balls to equilibrate between the P state and the S states. Equation (18) implies that $N_P+N_S=N$, where N is the total number of balls. Using this relation to eliminate N_S from the first expression of Eq. (20) gives

$$\dot{N}_P = \frac{p_{SP}v_S}{a}N - \frac{(p_{SP}v_S+2p_{PS}v_P)}{a}N_P. \tag{24}$$

Using Eqs. (16) and (22), this means that the time τ_{PS} for the equilibration of P and S energy is given by

$$\tau_{PS} = \frac{2l_P v_P^2}{(v_S^3+2v_P^3)}. \tag{25}$$

Trégourès and van Tiggelen [21] derived the same expression from the diffusion equation.

The equilibration among the two S states can be found by taking the difference of the last two lines of the system (15); this gives

$$\frac{d}{dt}(N_{S_1}-N_{S_2}) = -\frac{(2p_{SS}+p_{SP})v_S}{a}(N_{S_1}-N_{S_2}). \tag{26}$$

Note that the equilibration of the S states depends not only on the transition probability p_{SS} for the conversion between the S states, but also on the probability p_{SP} for the conversion between the P state and the S states. This is because conversions such as $S_1\to P\to S_2$ also contribute to the equilibration of the S states. With relations (16) and (17), it follows that the equilibration time τ_{SS} for the S states is given by

$$\tau_{SS}=\frac{l_S l_P}{l_P+(l_S/2)}\frac{1}{v_S}. \tag{27}$$

The model presented here does not account for the spatial variations in the ratio of the P- and S-wave energies. When this ratio has significant spatial variations the model cannot be expected to be accurate. Therefore the model is used in the following to describe the properties of the wave field after an equilibrium between the P- and S-wave propagation has been reached.

IV. PARTITIONING OF *P* AND *S* PROPAGATION

The analogy in Sec. III of balls that are distributed among different modes serves here as a simple model for the propagation of P and S waves in an elastic medium by identifying the propagation of balls in the P and S modes with the P- and S-wave energies, respectively. It is shown in Sec. II that in coda wave interferometry one measures averages of the propagation properties of the wave field with the squared amplitude of the waves, and hence the energy, as weight factor. This means that, according to expression (23), once the P and S waves have equilibrated the ratio of the time t_P spent traveling as a P wave to the time t_S that the wave traveled as an S wave is given by

$$\frac{t_P}{t_S}=\frac{v_S^3}{2v_P^3}. \tag{28}$$

This expression should be interpreted as an energy-weighted average after equilibration of the P- and S-wave energies.

The total travel time is given by $t_P+t_S=t$. With Eq. (28) this gives

$$t_S=\frac{2v_P^3}{2v_P^3+v_S^3}t,\quad t_P=\frac{v_S^3}{2v_P^3+v_S^3}t. \tag{29}$$

The meandering distance traveled as a P wave is given by $L_P=v_P t_P$ and the corresponding distance for the S waves is $L_S=v_S t_S$, so that

$$L_S=\frac{2v_P^3 v_S}{2v_P^3+v_S^3}t,\quad L_P=\frac{v_P v_S^3}{2v_P^3+v_S^3}t. \tag{30}$$

The total length of the wandering path is given by $L=L_S+L_P$, so that

$$L=\frac{2v_P^3 v_S+v_P v_S^3}{2v_P^3+v_S^3}t. \tag{31}$$

This means that after the P and S waves have equilibrated they propagate on average with an effective velocity $v_{\rm eff}$ that is given by

$$v_{\rm eff}=\frac{v_P v_S(2v_P^2+v_S^2)}{2v_P^3+v_S^3}. \tag{32}$$

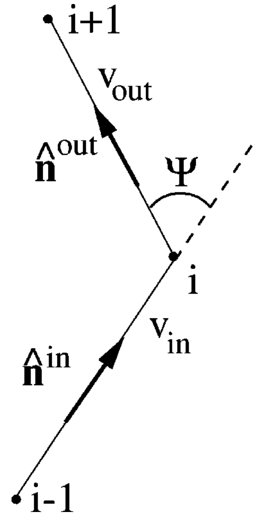

FIG. 2. Definition of the scattering angle and parameters of the incoming and outgoing waves at scatter i.

For a Poisson medium $v_{\rm eff}\approx 1.064 v_S$, so that the effective velocity is close to the S velocity.

The number of scatterers encountered is given by $n=L_S/l_S+L_P/l_P$; therefore from Eqs. (29) and (30) it follows that

$$n=\frac{v_P v_S}{2v_P^3+v_S^3}\left(\frac{2v_P^2}{l_S}+\frac{v_S^2}{l_P}\right)t. \tag{33}$$

Writing the number of scatterers as

$$n=\frac{v_{\rm eff}}{l_{\rm eff}}t, \tag{34}$$

this gives for the effective mean free path

$$\frac{1}{l_{\rm eff}}=\frac{1}{2v_P^2+v_S^2}\left(\frac{2v_P^2}{l_S}+\frac{v_S^2}{l_P}\right). \tag{35}$$

V. PERTURBING THE SCATTERER LOCATIONS

In this section, I derive the influence of random perturbations of the scatterer locations on the time-windowed correlation function. The perturbations of the components of the scatterer locations are assumed to be independent with zero

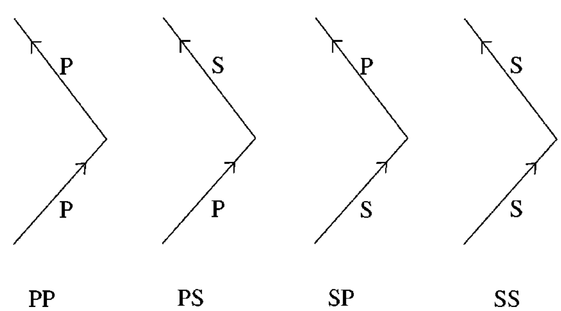

FIG. 3. Diagram of the four pairs of incoming and outgoing wave types at a scatterer.

mean and variance δ^2. Since the resulting mean travel time perturbation vanishes, the change in the correlation function is determined by the variance σ_τ^2 of the arrival times. This quantity can be retrieved from the data with expression (14). The elastic waves that propagate through the medium consist of both *P* and *S* waves; therefore, it is necessary to account for the possibility that the incoming and outgoing waves at a given scatterer are of different type. In the Appendix, I show that when the incoming wave at a given scatterer has velocity $v_{\rm in}$ and the outgoing wave a velocity $v_{\rm out}$, the variance in the arrival time due to the perturbation of a single scatterer location is given by

$$\sigma_\tau^2 = 2\delta^2\left(\frac{1}{2v_{\rm out}^2}+\frac{1}{2v_{\rm in}^2}-\frac{1}{v_{\rm out}v_{\rm in}}\cos\psi\right), \tag{36}$$

where ψ is the scattering angle of the trajectory as defined in Fig. 2.

This expression is valid for a perturbation of the location of one scatterer only. As shown in Fig. 3 for a given scatterer, there are four possibilities for the incoming and outgoing wave types because both the incoming and outgoing waves can be either a *P* or *S* wave. This means that expression (36) must be averaged, over these four types of incoming and outgoing waves, using the energy of the waves as weight factors. Applying this weighting to the relative occurrence of *P* and *S* trajectories gives a weight $2(v_P/v_S)^3$ to an *S*-wave trajectory relative to a *P*-wave trajectory. An *S* trajectory thus has a weight $v_S^3/(v_S^3+2v_P^3)$ while a *P* trajectory has a weight $2v_P^3/(v_S^3+2v_P^3)$. This gives the following weighting for products of the relative occurrences of pairs of incoming and outgoing trajectories shown in Fig. 3:

$$\begin{aligned} PP&: \quad v_S^6/(v_S^3+2v_P^3)^2,\\ PS&: \quad 2v_P^3v_S^3/(v_S^3+2v_P^3)^2,\\ SP&: \quad 2v_P^3v_S^3/(v_S^3+2v_P^3)^2,\\ SS&: \quad 4v_P^6/(v_S^3+2v_P^3)^2. \end{aligned} \tag{37}$$

These weight factors are used to average Eq. (36) over the four combinations of incoming and outgoing waves. For *n* scatterers along a trajectory, the variance σ_τ^2 is multiplied by *n* because the perturbations of the scatterer location are assumed to be independent. This gives for the variance in the arrival time

$$\begin{aligned}\sigma_\tau^2 = 2n\delta^2\Bigg\{&\frac{v_S^6}{(v_S^3+2v_P^3)^2}\left(\frac{1}{2v_P^2}+\frac{1}{2v_P^2}-\frac{1}{v_P^2}\langle\cos\psi_{PP}\rangle\right)+\frac{2v_P^3v_S^3}{(v_S^3+2v_P^3)^2}\left(\frac{1}{2v_S^2}+\frac{1}{2v_P^2}-\frac{1}{v_Sv_P}\langle\cos\psi_{SP}\rangle\right)+\frac{2v_P^3v_S^3}{(v_S^3+2v_P^3)^2}\left(\frac{1}{2v_P^2}\right.\\ &\left.+\frac{1}{2v_S^2}-\frac{1}{v_Pv_S}\langle\cos\psi_{SP}\rangle\right)+\frac{4v_P^6}{(v_S^3+2v_P^3)^2}\left(\frac{1}{2v_S^2}+\frac{1}{2v_S^2}-\frac{1}{v_S^2}\langle\cos\psi_{SS}\rangle\right)\Bigg\}.\end{aligned} \tag{38}$$

In this expression $\langle\cos\psi_{SP}\rangle$ is the average of the cosine of the scattering angle for *S* to *P* scattering over all scattering angles because the multitude of paths that visit a given scatterer sample all possible scattering angles. From reciprocity, $\langle\cos\psi_{SP}\rangle=\langle\cos\psi_{PS}\rangle$.

Expression (33) relates the average number of scatterers encountered to the travel time along the trajectory, taking conversions between *P* and *S* waves into account. Using this result to eliminate *n* from Eq. (38), the variance of the travel time is given by

$$\sigma_\tau^2=\frac{2\delta^2 t}{v_* l_*}, \tag{39}$$

with the velocity v_* given by

$$\frac{1}{v_*}\equiv\frac{2v_P^2+v_S^2}{(2v_P^3+v_S^3)^3}\left(\frac{v_S^7}{v_P}+2v_S^4v_P^2+2v_S^2v_P^4+4\frac{v_P^7}{v_S}\right), \tag{40}$$

and the transport mean free path given by

$$\frac{1}{l_*}\equiv\frac{1}{l_{\rm eff}}\left(1-\frac{(v_S^6/v_P^2)\langle\cos\psi_{PP}\rangle+4v_P^2v_S^2\langle\cos\psi_{PS}\rangle+4(v_P^6/v_S^2)\langle\cos\psi_{SS}\rangle}{v_S^6/v_P^2+2v_Pv_S^3+2v_P^3v_S+4v_P^6/v_S^2}\right), \tag{41}$$

with the effective mean free path $l_{\rm eff}$ given by Eq. (35).

Equation (39) is identical to the expression for the travel time variance for scalar waves [11,32]. This means that the change in the arrival time (or phase) caused by perturbations in scatterer locations has the same functional form for both elastic and scalar waves, despite the recurrent conversions between *P* and *S* waves. Note that these expressions are based on the presence of two *S* polarizations. For a twodimensional elastic medium the expressions for v_* and l_* are different.

For a Poisson medium, v_* and l_* are given by

$$v_* \approx 1.005 v_S, \tag{42}$$

and

$$\frac{1}{l_*} \approx \frac{1}{l_{\text{eff}}} (1 - 0.003 \langle \cos \psi_{PP} \rangle - 0.098 \langle \cos \psi_{PS} \rangle - 0.883 \langle \cos \psi_{SS} \rangle). \tag{43}$$

Note that the velocity v_* is close to the S velocity, and that the transport mean free path depends most strongly on the scattering angle for S waves because when the P and S waves have equilibrated the S waves are much more prolific. In fact, the error is not large when one replaces v_* by the S velocity and ignores in expression (43) the contributions of the scattering angles ψ_{PP} and ψ_{PS} that involve the P wave.

By inserting Eq. (39) in Eq. (14) we can relate the variance in the scatterer displacement to the time-windowed correlation function:

$$\delta^2 = (1 - R_{\max}^{(t,t_w)}) \frac{v_* l_*}{\overline{\omega^2} t}. \tag{44}$$

VI. A VELOCITY PERTURBATION

The change in the coda waves can be caused by a perturbation in the average velocity of the medium. Here, I derive the effect of constant perturbations of the P and S velocities on the time-windowed correlation of the coda waves. The relative perturbations of the P and S velocities are denoted by

$$\gamma_P \equiv \frac{\delta v_P}{v_P}, \quad \gamma_S \equiv \frac{\delta v_S}{v_S}. \tag{45}$$

For the equilibration model for P and S waves of Sec. IV, along each trajectory, the wave spends on average a time t_S as an S wave and a time t_P as a P wave. The unperturbed travel time is given by

$$t = \frac{L_P}{v_P} + \frac{L_S}{v_S}. \tag{46}$$

If we assume that the relative velocity perturbations are much smaller than unity, the average change in the arrival time, to first order in γ_P and γ_S, is given by

$$\langle \tau \rangle_{(t,t_w)} = -\gamma_P \frac{L_P}{v_P} - \gamma_S \frac{L_S}{v_S}. \tag{47}$$

Using expression (30) gives

$$\langle \tau \rangle_{(t,t_w)} = -\frac{1}{2v_P^3 + v_S^3} (v_S^3 \gamma_P + 2 v_P^3 \gamma_S) t. \tag{48}$$

The relative change in the effective velocity is related to the mean travel time perturbation by

$$\gamma_{\text{eff}} = -\frac{\langle \tau \rangle_{(t,t_w)}}{t} = \frac{v_S^3}{2v_P^3 + v_S^3} \frac{\delta v_P}{v_P} + \frac{2v_P^3}{2v_P^3 + v_S^3} \frac{\delta v_S}{v_S}. \tag{49}$$

Coda wave interferometry thus constrains the weighted average of the P- and S-velocity perturbation given by expression (49). For a Poisson medium

$$\gamma_{\text{eff}} \approx 0.09 \frac{\delta v_P}{v_P} + 0.91 \frac{\delta v_S}{v_S}, \tag{50}$$

so that coda wave interferometry for elastic waves depends much more strongly on the relative perturbation of the S-wave velocity than on that of the P-wave velocity.

VII. CONCLUSION

The treatment of coda wave interferometry as formulated for scalar waves extends to that of elastic waves, which are subject to the conversion between P and S waves. The resulting expressions for the time-windowed correlation function of the multiple-scattered waves due to changes of the medium are identical to those previous derived for scalar waves. Coda wave interferometry for elastic waves differs from that for scalar waves only in that it depends on a weighted average of the propagation and scattering properties of P and S waves. In practice, elastic coda wave interferometry is predominantly influenced by the propagation and scattering of S waves because these waves dominate over the P waves after multiple scattering. Therefore this technique is most sensitive to changes in the propagation characteristics of S waves [17].

ACKNOWLEDGMENTS

I greatly appreciate the critical comments of Ken Larner, Matt Haney, and Huub Douma. This work was supported by the NSF (Grant No. EAR-0106668) and by the sponsors of the Consortium Project on Seismic Inverse Methods for Complex Structures at the Center for Wave Phenomena.

APPENDIX: THE EFFECT OF THE PERTURBATION OF ONE SCATTERER LOCATION ON THE TRAVEL TIME

Consider the situation shown in Fig. 2 wherein the location of scatterer i is perturbed, while the locations of the scatterers $i-1$ and $i+1$ that the wave encounters before and after meeting scatterer i, respectively, are unperturbed. The incoming wave travels from scatterer $i-1$ to scatterer i with velocity v_{in} in the direction $\hat{\mathbf{n}}^{\text{in}}$ and the outgoing wave from scatterer i to $i+1$ travels with velocity v_{out} in the direction $\hat{\mathbf{n}}^{\text{out}}$. The location of scatterer i is denoted by $\mathbf{r}^{(i)}$. The three components of this vector are perturbed independently with zero mean and variance δ.

It follows by differentiation that $\partial |\mathbf{r}^{(i+1)} - \mathbf{r}^{(i)}| / \partial x^{(i)} = -(x^{(i+1)} - x^{(i)}) / |\mathbf{r}^{(i+1)} - \mathbf{r}^{(i)}| = -\hat{n}_x^{\text{out}}$. Using this, and the corresponding result for the incoming wave, gives for the travel time t

$$\frac{\partial t}{\partial x_i} = -\frac{1}{v_{\mathrm{out}}}\hat{n}_x^{\mathrm{out}} + \frac{1}{v_{\mathrm{in}}}\hat{n}_x^{\mathrm{in}}, \tag{A1}$$

with similar expressions for the other derivatives. Since the perturbations in the three components of the location of scatterer i are assumed to be independent, the associated variance in the travel time is given by $\langle \tau^2 \rangle_i = (\partial t/\partial x_i)^2 \delta^2 + (\partial t/\partial y_i)^2 \delta^2 + (\partial t/\partial z_i)^2 \delta^2$. With expression (A1) this gives expression (36).

[1] J. F. Claerbout, *Imaging the Earth's Interior* (Blackwell, Oxford, 1985).

[2] K. J. Langenberg, R. Marklein, and K. Mayer, in *Scattering and Inverse Scattering in Pure and Applied Science*, edited by P. C. Sabatier and E. R. Pike (Academic, San Diego, 2002).

[3] J. A. Jensen, in *Imaging of Complex Media with Acoustic and Seismic Waves*, edited by M. Fink, W. A. Kuperman, J. P. Montagner, and A. Tourin (Springer, Berlin, 2002), pp. 135–165.

[4] N. A. Fomin, *Speckle Photography for Fluid Mechanics Measurements* (Springer, Berlin, 1998).

[5] M. Heckmeier and G. Maret, Prog. Colloid Polym. Sci. **104**, 12 (1997).

[6] T. Okamato and T. Asakura, Prog. Opt. **34**, 183 (1995).

[7] Ping Sheng, *Introduction to Wave Scattering, Localization, and Mesoscopic Phenomena* (Academic, San Diego, 1995).

[8] G. Maret and P. E. Wolf, Z. Phys. B: Condens. Matter **65**, 409 (1987).

[9] W. Leutz and G. Maret, Physica B **204**, 14 (1995).

[10] D. Bicout and G. Maret, Physica A **210**, 87 (1994).

[11] R. Snieder, A. Grêt, H. Douma, and J. Scales, Science **295**, 2253 (2002).

[12] G. Poupinet, W. L. Ellsworth, and J. Frechet, J. Geophys. Res. B **89**, 5719 (1984).

[13] A. Ratdomopurbo and G. Poupinet, Geophys. Res. Lett. **22**, 775 (1995).

[14] D. A. Dodge and G. C. Beroza, J. Geophys. Res., [Solid Earth] **102**, 24437 (1997).

[15] Y. G. Li, J. E. Vidale, K. Aki, F. Xu, and T. Burdette, Science **279**, 217 (1998).

[16] T. Nishimura, N. Uchida, H. Sato, M. Ohtake, S. Tanaka, and H. Hamaguchi, Geophys. Res. Lett. **27**, 269 (2000).

[17] K. Aki and L. B. Chouet, J. Geophys. Res. **80**, 3322 (1975).

[18] R. L. Weaver, J. Acoust. Soc. Am. **71**, 1608 (1982).

[19] D. M. Egle, J. Acoust. Soc. Am. **70**, 476 (1981).

[20] G. Papanicolaou and L. Ryzhik, IAS/Park City Math. Ser. **5**, 307 (1999).

[21] N. P. Trégourès and B. A. van Tiggelen, Waves Random Media **12**, 21 (2002).

[22] M. Campillo, L. Margerin, and N. M. Shapiro, in *Diffuse Waves in Complex Media*, edited by J. P. Fouque (Kluwer, Dordrecht, 1999), pp. 383–404.

[23] S. Chandrasekhar, *Radiative Transfer* (Dover, New York, 1960).

[24] R. S. Wu, Geophys. J. R. Astron. Soc. **82**, 57 (1985).

[25] J. A. Turner and R. L. Weaver, J. Acoust. Soc. Am. **96**, 3654 (1994).

[26] L. Ryzhik, G. C. Papanicolaou, and J. B. Keller, Commun. Partial Differ. Eqns. **22**, 1869 (1997).

[27] L. Margerin, M. Campillo, and B. van Tiggelen, Geophys. J. Int. **134**, 596 (1998).

[28] P. Morse and H. Feshbach, *Methods of Theoretical Physics, Part 1* (McGraw-Hill, New York, 1953).

[29] K. Yoshimoto, J. Geophys. Res., [Solid Earth] **105**, 6153 (2000).

[30] L. Margerin, M. Campillo, and B. van Tiggelen, J. Geophys. Res., [Solid Earth] **105**, 7873 (2000).

[31] K. Aki, Bull. Seismol. Soc. Am. **82**, 1969 (1992).

[32] R. Snieder and J. A. Scales, Phys. Rev. E **58**, 5668 (1998).